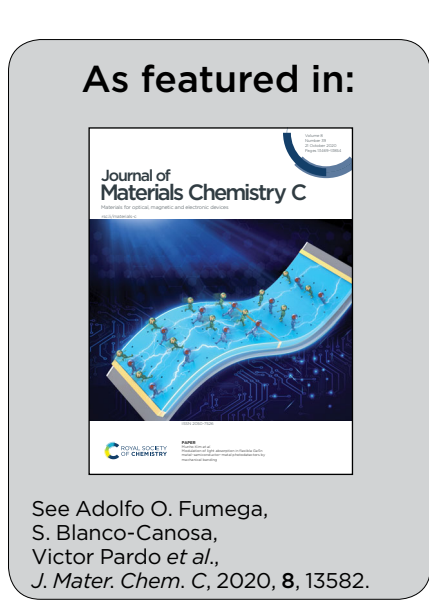


Showcasing collaborative research from The University of Santiago de Compostela, Spain; Donostia International Physics Center, Spain; The University of Texas at Austin, USA; and ALBA Synchrotron Light Source, Spain.

Electronic structure and magnetic exchange interactions of Cr-based van der Waals ferromagnets. A comparative study between  $CrBr_3$  and  $Cr_2Ge_2Te_6$ 

Ab initio calculations and high-pressure experiments unveil the microscopic mechanism behind the magnetic properties of two Cr-based van der Waals ferromagnets that have different electronic structure.





## Journal of Materials Chemistry C



PAPER

View Article Online
View Journal | View Issue



**Cite this:** *J. Mater. Chem. C*, 2020, **8**, 13582

# Electronic structure and magnetic exchange interactions of Cr-based van der Waals ferromagnets. A comparative study between CrBr<sub>3</sub> and Cr<sub>2</sub>Ge<sub>2</sub>Te<sub>6</sub>†

Adolfo O. Fumega, \*\*D \*\* S. Blanco-Canosa, \*\*Cd H. Babu-Vasili, \*\* P. Gargiani, \*\* Hongze Li, \*\*Jian-Shi Zhou, \*\* F. Rivadulla \*\*D \*\*g and Victor Pardo\*\*ab

Low dimensional magnetism has been powerfully boosted as a promising candidate for numerous applications. The stability of the long-range magnetic order is directly dependent on the electronic structure and the relative strength of the competing magnetic exchange constants. Here, we report a comparative pressure-dependent theoretical and experimental study of the electronic structure and exchange interactions of two-dimensional ferromagnets CrBr<sub>3</sub> and Cr<sub>2</sub>Ge<sub>2</sub>Te<sub>6</sub>. While CrBr<sub>3</sub> is found to be a Mott–Hubbard-like insulator, Cr<sub>2</sub>Ge<sub>2</sub>Te<sub>6</sub> shows a charge-transfer character due to the broader character of the Te 5p bands at the Fermi level. This different electronic behaviour is responsible for the robust insulating state of CrBr<sub>3</sub>, in which the magnetic exchange constants evolve monotonically with pressure, and the proximity to a metal–insulator transition predicted for Cr<sub>2</sub>Ge<sub>2</sub>Te<sub>6</sub>, which causes a non-monotonic evolution of its magnetic ordering temperature. We provide a microscopic understanding for the pressure evolution of the magnetic properties of the two systems.

Received 23rd April 2020, Accepted 22nd June 2020

DOI: 10.1039/d0tc02003f

rsc.li/materials-c

#### I. Introduction

Two-dimensional (2D) materials have increased their academic and technological relevance continuously since the successful synthesis of graphene in 2004.<sup>1</sup> Many other materials, like transition metal dichalcogenides, <sup>2</sup> boron nitride (BN)<sup>3</sup> or phosphorene, have been profusely studied since then.<sup>4</sup> Recently, long-range ferromagnetic (FM) order in several atomic-thick materials, such as FePS<sub>3</sub>, <sup>5</sup> CrI<sub>3</sub> <sup>6</sup> and itinerant Fe<sub>3</sub>GeTe<sub>2</sub> <sup>7</sup> has been reported. The advent of long-range 2D ferromagnetism

brings about new transport phenomena in two dimensions, like

Layered van der Waals materials provide a unique platform to study the evolution of the magnetic exchange interactions when going from the 2D to the 3D limit. In particular, Cr-based van der Waals ferromagnets have gained attention over the past years due to their high magnetic moment and Curie temperature. In these compounds, magnetic order is determined by different exchange paths. For instance, the isotropic in-plane magnetic coupling  $J_{\rm in}$  in transition metal dichalcogenides (TMDs), di- and trihalides and phosphosulfides, is determined by the competition between metal–metal direct exchange and indirect exchange mediated by the anions. These exchange paths have been found to be highly dependent on the crystal and electronic structure, and different strategies have been proposed to tune them. Is, 16

 ${\rm CrBr_3}$  and  ${\rm Cr_2Ge_2Te_6}$  crystallize in a lamellar structure with hexagonal symmetry (space group no. 148), forming a honeycomb network of edge-sharing octahedra, stacked with van der Waals gaps separating the  ${\rm Cr^{3^+}}$ -rich planes, as shown in Fig. 1. Both compounds retain their bulk ferromagnetism down to the single layer limit,  $T_{\rm C}=34~{\rm K}$  for  ${\rm CrBr_3}$  and  $T_{\rm C}=61$  for  ${\rm Cr_2Ge_2Te_6}$ ,

tunneling magnetoresistance<sup>8,9</sup> and electrical switching of magnetic states,<sup>10</sup> promoting 2D ferromagnets as versatile platforms for engineering new quantum states and device functionalities. Besides, 2D materials can exhibit multitude of exotic properties when combined in heterostructures.<sup>11</sup>

Layered van der Waals materials provide a unique platform

 <sup>&</sup>lt;sup>a</sup> Departamento de Física Aplicada, Universidade de Santiago de Compostela,
 E-15782 Campus Sur s/n, Santiago de Compostela, Spain.
 E-mail: adolfo.otero.fumega@usc.es, victor.pardo@usc.es

b Instituto de Investigacións Tecnolóxicas, Universidade de Santiago de Compostela, E-15782 Campus Sur s/n, Santiago de Compostela, Spain

<sup>&</sup>lt;sup>c</sup> Donostia International Physics Center, DIPC, 20018 Donostia-San Sebastian, Basque Country, Spain. E-mail: sblanco@dipc.org

 $<sup>^</sup>d$  IKERBASQUE, Basque Foundation for Science, 48013 Bilbao, Basque Country, Spain

<sup>&</sup>lt;sup>e</sup> ALBA Synchrotron Light Source, Cerdanyola del Vallès, 08290 Barcelona, Catalonia. Spain

<sup>&</sup>lt;sup>f</sup> Texas Materials Institute, ETC 9.102, The University of Texas at Austin, Austin, Texas, 78712, USA

g CIQUS, Centro de Investigación en Química Biolóxica e Materiais Moleculares, and Departamento de Química-Física, Universidade de Santiago de Compostela, 15782-Santiago de Compostela, Spain

 $<sup>\</sup>dagger$  Electronic supplementary information (ESI) available. See DOI: 10.1039/d0tc02003f

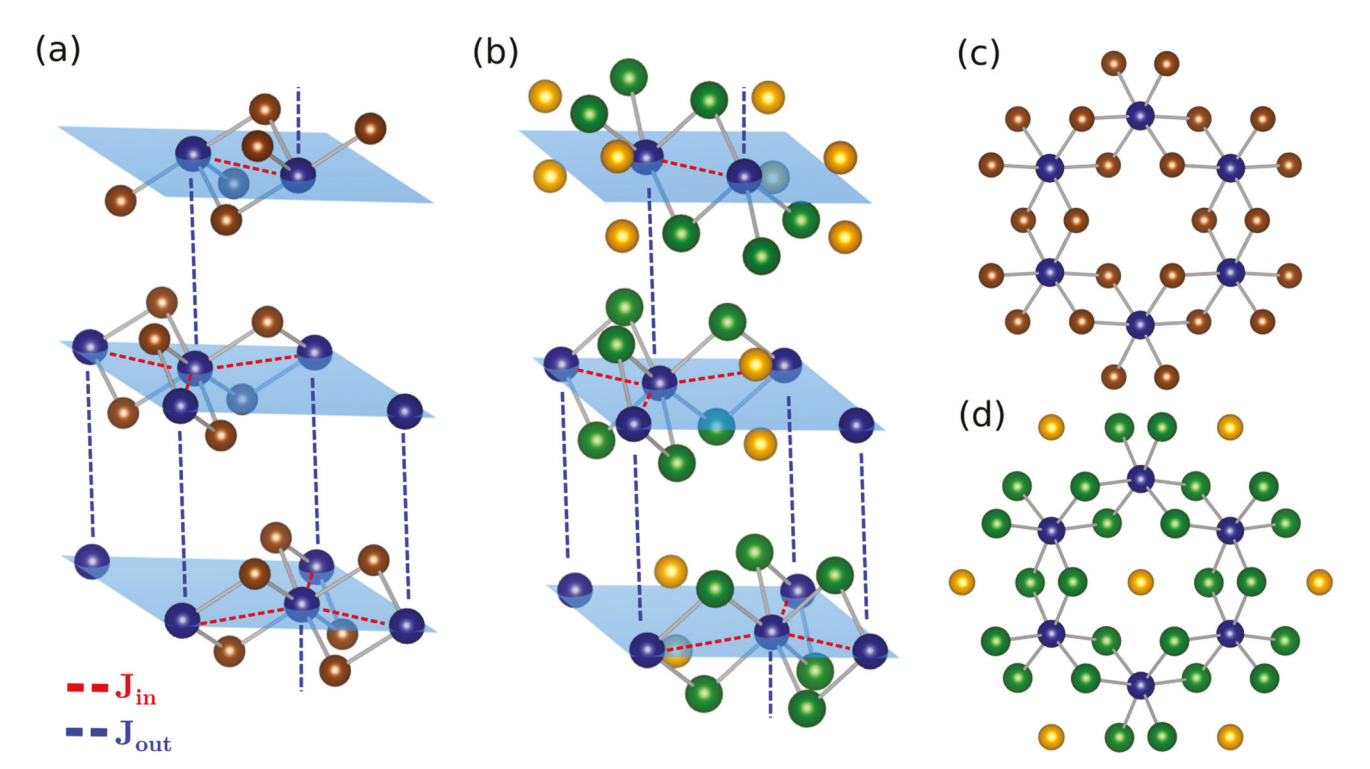


Fig. 1 Unit cells of (a) CrBr<sub>3</sub> and (b) Cr<sub>2</sub>Ge<sub>2</sub>Te<sub>6</sub>. Cr atom in blue, Br atom in brown, Ge atom in yellow and Te atom in green. Different exchange constants are considered: an in-plane Jin that takes into account both the direct Cr-Cr exchange and the superexchange via Br or Te, and the out-ofplane  $J_{out}$  that couples out-of-plane Cr-Cr neighbours. (c) and (d) Show the top view of CrBr<sub>3</sub> and Cr<sub>2</sub>Ge<sub>2</sub>Te<sub>6</sub> unit cells, respectively.

with an out-of-plane easy axis. 17-20 This magnetic anisotropy is necessary to circumvent the restrictions of the Mermin-Wagner theorem, leading to a long-range FM order at the monolayer limit. Therefore, the stabilization of 2D magnetic order requires a comprehensive understanding of the magnetic exchange interactions and their evolution as a function of order parameters like dimensionality or external pressure. By combining ab initio calculations and high-pressure experiments on single crystals of CrBr3 and Cr2Ge2Te6, we explore their electronic structure, and the pressure dependence of the in- and out-ofplane exchange interactions,  $J_{in}$  and  $J_{out}$ , (shown in Fig. 1). The pressure dependence of the magnetization measurements shows a different trend of the magnetic transition temperature,  $T_{\rm C}$ , for each compound. Our density-functional-theory-based calculations indicate that, while the evolution of  $T_{\rm C}$  at low pressures is driven by progressive decrease of  $J_{\rm in}$  for both systems, Jout is the dominant interaction in Cr<sub>2</sub>Ge<sub>2</sub>Te<sub>6</sub> at high pressure. We argue that the electronic band structure is responsible for the pressure evolution of the magnetic transition temperatures in each compound. Our work highlights the crucial role of electronic band structure to search for new materials retaining a large Curie temperature down to the monolayer limit.

The paper is organized as follows. In Section II, we describe the experimental and theoretical approaches used. Section III is devoted to report the electronic structure and magnetic exchange paths of both compounds, Section IV analyses the effect of dimensionality from the evolution of the electronic structure and magnetic properties under pressure. Finally, in Section V we provide a discussion of the results and a summary of the main conclusions of this work.

#### II. Computational and experimental procedures

Electronic structure ab initio calculations were performed within the density functional theory<sup>21,22</sup> framework using the all-electron, full potential code WIEN2K23 based on the augmented plane wave plus local orbital (APW + lo) basis set.<sup>24</sup> For the structural relaxations, in particular the computation of the lattice parameters at different pressures, special exchangecorrelation functionals were needed to deal with the out-ofplane van der Waals-type forces.<sup>25</sup> The exchange-correlation term chosen to compute the exchange parameters was the generalized gradient approximation (GGA) in the Perdew-Burke-Ernzerhof scheme which is found to provide a good description of the electronic structure and magnetism.<sup>26</sup> A fully-converged k-mesh of  $R_{\text{mt}}K_{\text{max}} = 7.0$  and muffin-tin radii of 2.42 a.u. for Cr, 2.07 a.u. for Ge, 2.19 a.u. for Br and 2.38 a.u. for Te, nicely converged with respect to all the input parameters in the simulations. Besides, the Curie temperature  $(T_C)$  at each pressure was obtained using 864 particles within a nearestneighbour Heisenberg model, with the exchange parameters mapped by the Monte Carlo Metropolis algorithm.<sup>27</sup> We have applied periodic boundary conditions and 106 steps in total. The  $T_{\rm C}$  was obtained by fitting the magnetization curves as explained in ref. 28.

Single crystals of  $CrBr_3$  and  $Cr_2Ge_2Te_6$  were synthesized from the purely elemental starting materials and provided by HQ graphene. The quality of the crystals was confirmed by X-ray diffraction and X-ray photoemission spectroscopy (XPS). X-ray absorption (XAS) and X-ray magnetic circular dichroism (XMCD) measurements up to 6 Tesla were performed at  $Cr L_{2,3}$  edge at the BOREAS BL29 beamline at ALBA synchrotron. <sup>29</sup> Magnetic measurements under pressure up to P=1 GPa were performed in a Be–Cu cell, using a silicon oil as pressure medium, inside a MPMS SQUID from Quantum Design. The pressure was monitored *in situ* through the superconducting transition of a Sn pressure gauge. X-ray diffraction under pressure was carried out in a diamond anvil cell using 4:1 methanol:ethanol as pressure media. The pressure dependence of the lattice volume up to 5 GPa was fitted to the Birch–Murnaghan equation.

### III. Electronic structure and magnetism

In this section we will describe the electronic structure and magnetic interactions for both compounds. Fig. 2 shows the density of states computed with DFT for  $CrBr_3$  and  $Cr_2Ge_2Te_6$ . In both cases, the electronic structure of Cr can be well described as a  $Cr^{3+}$ : $d^3$  cation with S=3/2, the majority-spin  $t_{2g}$  bands being fully occupied. For  $CrBr_3$ , the states just below

and above the Fermi level have dominant Cr d character, thus suggesting a Mott insulator behaviour with a d-d energy gap (top panel in Fig. 2a). This result is in agreement with previous photoluminescence experiments.<sup>20</sup>

On the other hand, for  $Cr_2Ge_2Te_6$ , the states just below the Fermi level are very broad and have dominant Te p character. A p-d energy gap is observed for this material, which suggests a charge transfer insulator behaviour. Ge atoms do not play a substantial role in the electronic structure, with a vanishing contribution close to the Fermi level (top panel in Fig. 2b).

Fig. 3a shows the experimental isotropic XAS taken at 2 K for Cr<sub>2</sub>Ge<sub>2</sub>Te<sub>6</sub>. The isotropic spectrum is defined as the average of circular  $\sigma^-$  and circular  $\sigma^+$  polarized light. The two main peaks correspond to the  $2p_{3/2}$  (575 eV) and  $2p_{1/2}$  (585 eV) components of the 2p core level (split by spin-orbit coupling). The energy profile is comparable to Cr<sub>2</sub>O<sub>3</sub>, demonstrating a Cr<sup>3+</sup> oxidation state.<sup>30</sup> We have performed cluster calculations for the atomic-like  $2p^63d^3 \rightarrow 2p^53d^4$  transition for  $Cr^{3+}$  ( $C_{3v}$  symmetry) using the crystal field theory (CFT) implemented in QUANTY. 31,32 The method accounts for the intraatomic 3d-3d and 2p-3d coulomb and exchange interactions, the atomic 2p and 3d spin-orbit couplings and the local crystal field parameters  $D_q$ ,  $D_\sigma$  and  $D_\tau$ . We have adopted the values of U = 0 eV,  $F_{dd}^{0} = 0.805$  eV,  $F_{dd}^{2} = 15.61$  eV,  $F_{dd}^{4} = 15.61$  eV,  $F_{dd}^{4}$ 9.78 eV,  $F_{pd}^2 = 4.89$  eV,  $G_{pd}^1 = 2.22$  eV and  $G_{pd}^3 = 1.26$  eV as input of the Slater integrals. The calculated ground state is four-fold degenerate with spin quantum numbers  $S_z \sim \pm 3/2$  and  $\pm 1/2$ . The main

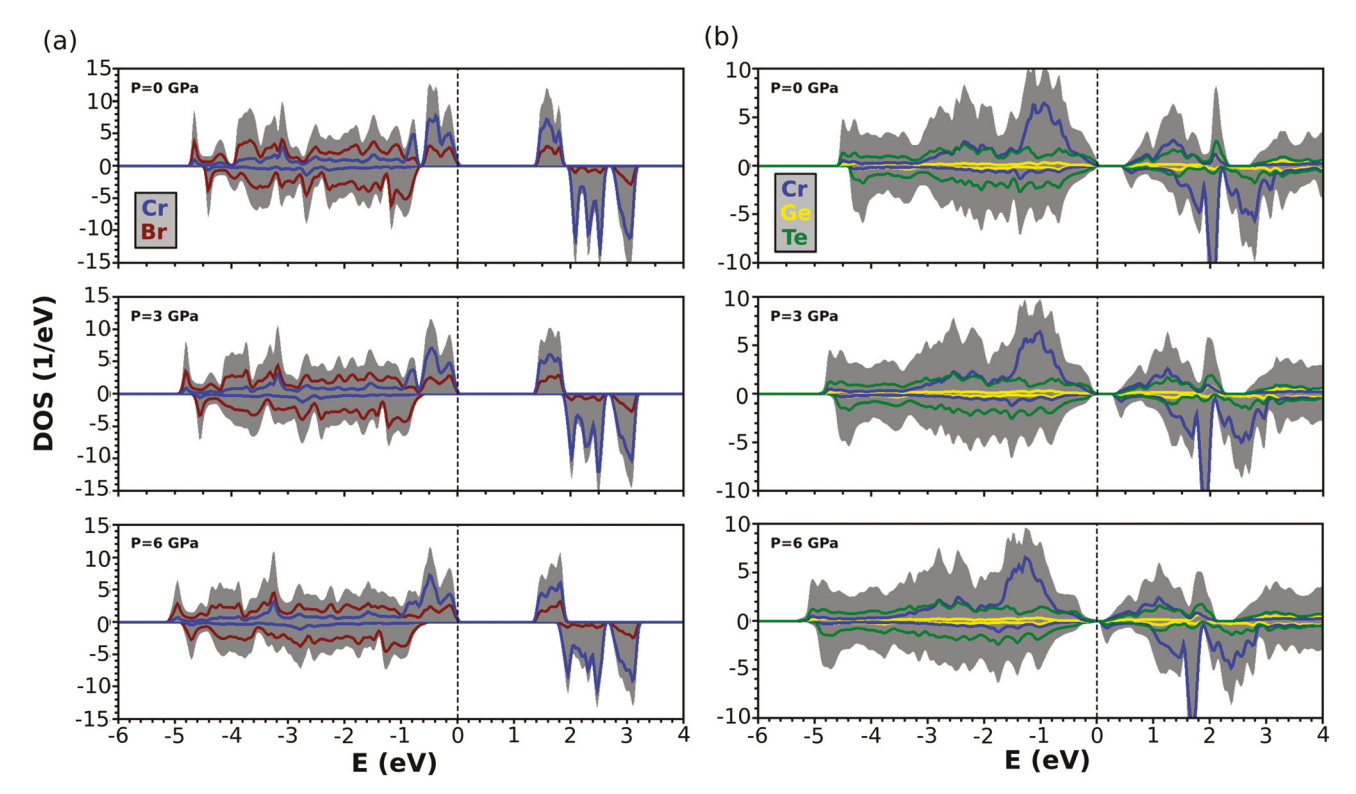
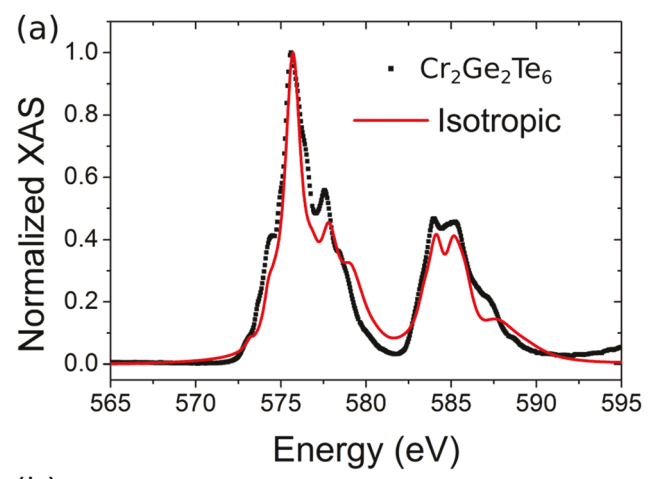


Fig. 2 Density of states as a function of pressure. The shaded area represents the total DOS, in positive (negative) the majority (minority) spin channel. Fermi energy was set to zero. (a) Partial density of states (DOS) of the Cr d (blue) and Br p (brown) states. The energy gap has d-d character. (b) Partial density of states (DOS) of the Cr d (blue), Ge p (yellow) and Te p (green) states. Note the large bandwidth of the Te p states leading to a substantial charge transfer; the larger weight at the Fermi level is due to Te p bands. The gap closes completely at high pressure in this case.



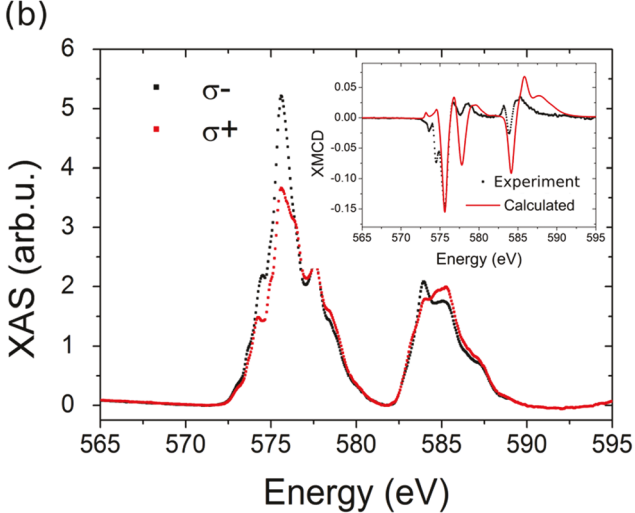


Fig. 3 (a) X-ray absorption of Cr<sub>2</sub>Ge<sub>2</sub>Te<sub>6</sub> at the Cr L-edge (black dots) and the calculated XAS spectra. (b) Experimental circular left (black) and right (red) polarized light. Inset, experimental and theoretical XMCD spectra for  $Cr^{3+}$  with  $C_{3v}$  symmetry.

features of the spectra are well modelled with cluster calculations despite the low symmetry of the Cr site and the mixing of L3 and L2 edges, assuming  $D_{\rm q} \sim 0.3$  eV,  $D_{\sigma} = 0$  eV and  $D_{\tau} = 0$  eV. In Fig. 3b, we show the  $\sigma^+$  and  $\sigma^-$  polarized light and the XMCD spectra (inset) defined as  $\sigma^- - \sigma^+$  together with the theoretical calculation. Again, the fitting reproduces the main peaks and splittings of the spectra, although the calculation does not model the low energy tail ( $\sim$  572 eV) of the XMCD spectrum (inset).

From the theoretical point of view, the different energy contributions to the magnetic ground state can be modelled separately by considering the nearest-neighbour  $J_{\rm in}$  and the  $J_{\rm out}$ exchange couplings (see ESI† for more details). Four more exchange paths including second and third nearest neighbours have been included in previous works.<sup>33</sup> Nevertheless, as we will discuss, our simple Heisenberg-type model suffices to explain the magnetic order as a function of pressure in these compounds. The different J's are shown in Fig. 1, with the  $J_{in}$ and J<sub>out</sub> depicted as broken red and blue lines, and the Cr<sup>3+</sup> cations surrounded by edge-sharing trigonally distorted octahedra.  $J_{\rm in}$  is the sum of two exchange contributions, the direct

Cr-Cr exchange across the octahedral edge, which is antiferromagnetic (AF) between two half-filled t2g bands, and the indirect Cr-(Br or Te)-Cr superexchange at approximately 90-degrees. According to Goodenough-Kanamori-Anderson rules, the indirect exchange, cation-anion-cation, can be either FM or AF, depending on the strength of the delocalization and correlation superexchange effects. <sup>12</sup> Our results show that  $J_{in}$  = 27.5 K and  $J_{\text{out}} = 12 \text{ K}$  for  $\text{Cr}_2\text{Ge}_2\text{Te}_6$  and  $J_{\text{in}} = 28.5 \text{ K}$  and  $J_{\text{out}} = 6 \text{ K}$  for CrBr3. These values were obtained by fitting total energy differences between different magnetic configurations to a Heisenbergtype Hamiltonian. All I's are positive, which explain the FM order observed in the experiments for both compounds. These results lead to theoretical Curie temperatures of 77 K for Cr<sub>2</sub>Ge<sub>2</sub>Te<sub>6</sub> and 69 K for CrBr3, this small overestimation is in the range of acceptable values for GGA.

Fig. 4 shows the magnetization vs. temperature at P = 0 GPa for CrBr<sub>3</sub> and up to 1 GPa for Cr<sub>2</sub>Ge<sub>2</sub>Te<sub>6</sub>. The magnetic transitions appear as an upturn in the magnetization upon cooling at 37 and 63 K, respectively, following a Curie-Weiss behavior at  $T > T_{\rm C}$ .

#### IV. Evolution with pressure

We have carried out ab initio calculations, complemented with high-pressure magnetic and X-ray diffraction measurements to study the evolution of the electronic structure and magnetic exchange interactions. Naively, one can interpret the effect of isotropic pressure on the magnetic exchange interactions as a smooth evolution from a 2D-toward a more 3D-like magnetic state, since the c-axis compressibility is expected to be much larger than that of the a-b plane.

Fig. 2 shows the DOS and the partial DOS (pDOS) as a function of pressure for both compounds. In Fig. 2a we see that CrBr<sub>3</sub> does not undergo a substantial modification of its electronic structure with pressure. The d-d energy gap observed at P = 0 GPa is preserved when pressure is raised up to 6 GPa (see Fig. 5a). However, Fig. 2b shows how the p-d energy gap of Cr<sub>2</sub>Ge<sub>2</sub>Te<sub>6</sub> closes as pressure is increased (see Fig. 5a). Therefore, our calculations predict that Cr<sub>2</sub>Ge<sub>2</sub>Te<sub>6</sub> undergoes an insulator to metal transition at high pressure. The values of the band gaps presented here were obtained using GGA, which has a tendency to underestimate them. This is less so when dealing with crystal-field gaps.34 Yet, the pressure evolution should be correct in any case.

Fig. 5b shows the pressure dependence of the cation-anioncation angle. While for the Mott insulator CrBr3 the angle shows a monotonic decrease up to 10 GPa, in Cr<sub>2</sub>Ge<sub>2</sub>Te<sub>6</sub> the angle remains constant in the whole range of pressures up to 10 GPa. Hence, external pressure modifies the internal structure of CrBr3, while in Cr2Ge2Te6, there is a pressure induced insulator to metal transition as a consequence of the closing of the energy gap due to the change in the Te-Cr distance and not the Cr-Te-Cr angle, which remains roughly unchanged.

In order to shed light on the nature of the pressure-induced metal-insulator transition predicted by our DFT calculations

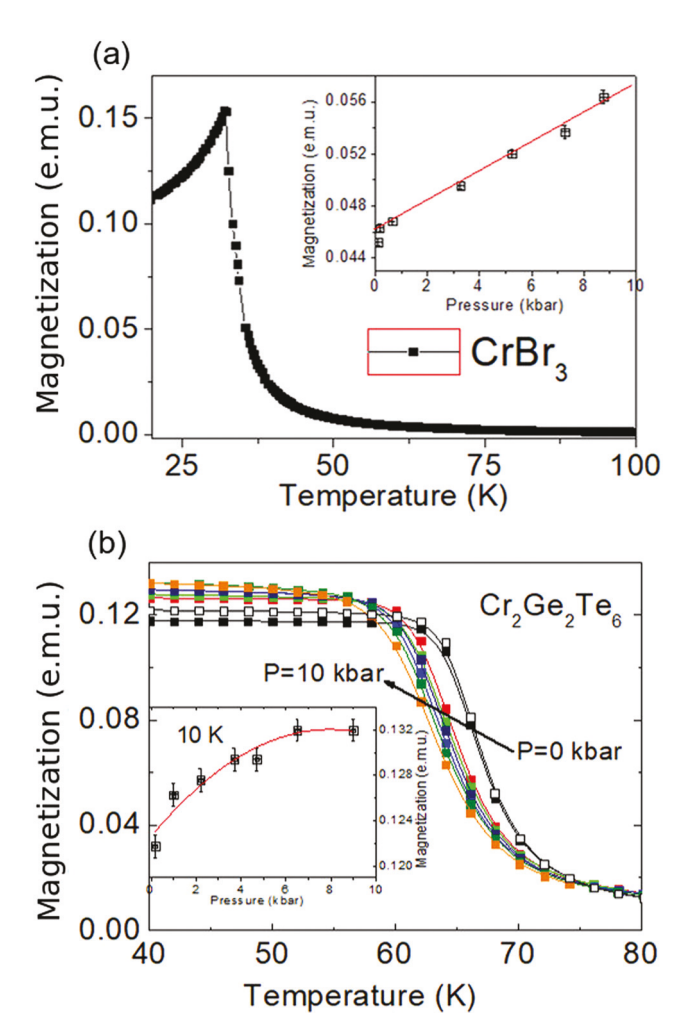


Fig. 4 (a) Magnetization vs. temperature at zero pressure for CrBr<sub>3</sub>, H=0.1 T. Inset: Linear pressure dependence of the magnetization at 10 K. (b) Temperature dependence of the magnetization (H=0.1 T) up to 1 GPa for Cr<sub>2</sub>Ge<sub>2</sub>Te<sub>6</sub>. Inset: Pressure dependence of the magnetization. At 10 K and above 6 kbar (0.6 GPa) the magnetization saturates in agreement with the pressure dependence of the in and out exchange interactions,  $J_{\text{in,out}}$ , see text. (Red lines are guides to eye).

for  $Cr_2Ge_2Te_6$ , we have performed high pressure X-ray diffraction (XRD) measurements. In Fig. 6, we plot the pressure dependence of the ratio of the lattice parameters, c/a, showing a sudden decrease above 7 GPa, suggesting a structural transition. This pressure coincides with the collapse of the electronic gap, as predicted by our *ab initio* calculations. The insulator to metal transition observed in our DFT calculations was obtained assuming that the symmetry of the lattice remains unchanged upon pressure. Pressure-induced structural phase transitions and amorphizations have been observed before by means of high pressure X-ray diffraction between 18 and 30 GPa for  $Cr_2Ge_2Te_6$ . However, no structural anomalies were reported at pressures relevant in this work.<sup>35</sup>

Fig. 4 and 7 display the evolution of the magnetic transition temperature of  $CrBr_3$  and  $Cr_2Ge_2Te_6$  up to 1 GPa. As seen in the raw data and summarized in Fig. 7, the  $T_C$  of both compounds decreases as pressure is applied, in agreement with previous

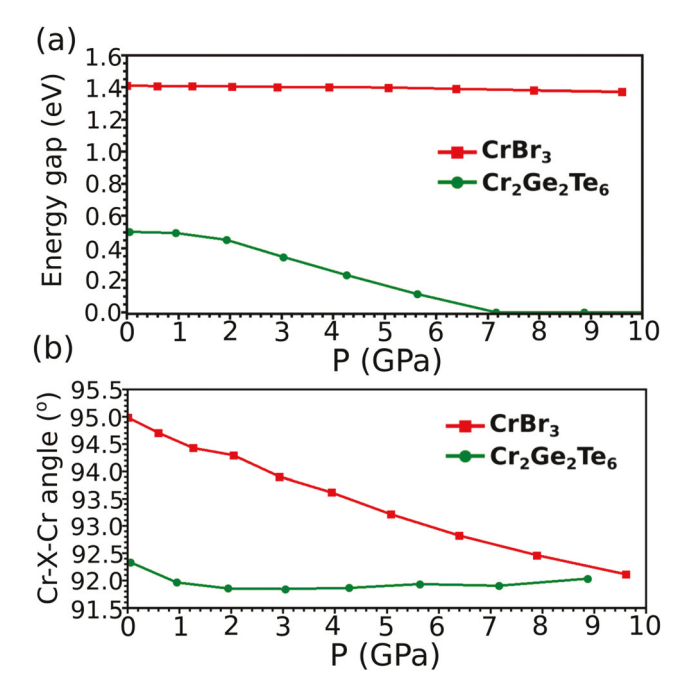
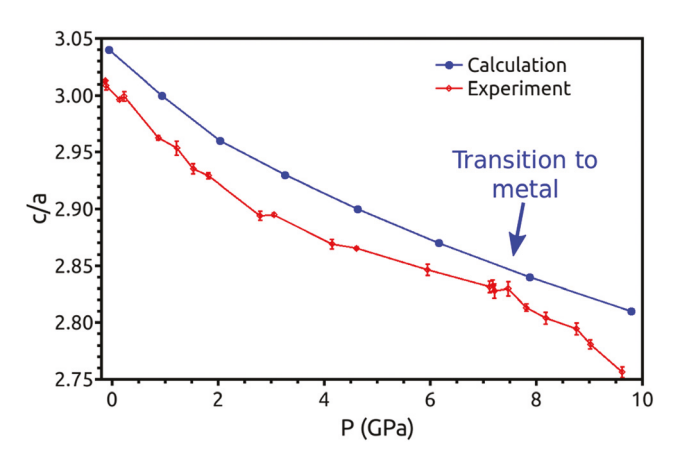


Fig. 5 (a) Calculated energy gap as a function of pressure for both compounds, obtained using the GGA exchange-correlation functional. (b) Evolution of the Cr-X-Cr angle as a function of pressure. X represents Br or Te atoms.



**Fig. 6** Comparison of the high pressure XRD data with the results of our *ab initio* calculation for the *c/a* ratio. DFT predicts a transition to a metallic state around the same pressure that XRD data shows a peak.

reports<sup>36,37</sup> and at odds with the expectations for the pressure dependence of the exchange interaction in a localized magnetic system. Harrison<sup>38</sup> stated that the transition temperature for a localized system increases as a function of the distance between magnetic sites as  $r^{-(l+l'+1)}$ , where l and l' are the angular momentum quantum numbers. This results in a variation of the magnetic exchange interaction with volume, J(V) as 3.3 and 4.6 for direct and indirect superexchange, respectively, the so-called Bloch's rule.<sup>39</sup> Violations of Bloch's rule have been observed in Mott insulators close to a metal–insulator<sup>40</sup> and spin-Peierls to Peierls<sup>41</sup> transitions. Bloch's rule describes the

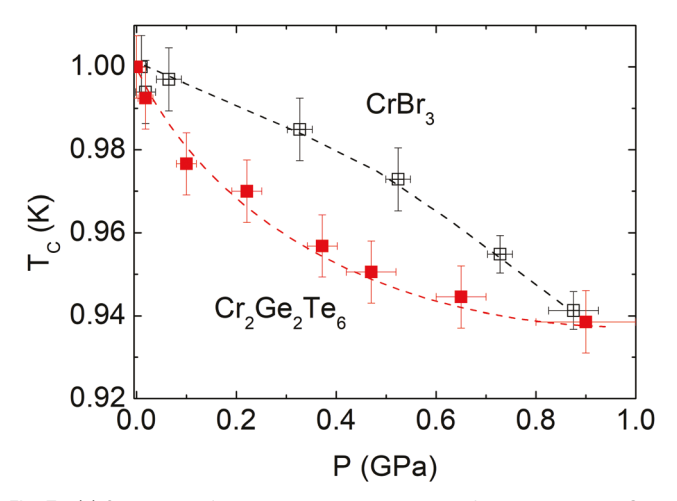


Fig. 7 (a) Summary of the pressure dependence of the normalized Curie temperature, T<sub>C</sub> for Cr<sub>2</sub>Ge<sub>2</sub>Te<sub>6</sub> and CrBr<sub>3</sub>.

evolution with pressure of only one exchange constant. As we have seen above, in this case there is a competition between exchange constants that evolve differently with pressure, and even the  $J_{\rm in}$  is in itself the addition of two competing exchange mechanisms. Our data also shows a different trend for  $T_{\rm C}(P)$ than the simple Bloch's rule prediction: while the critical temperature of CrBr3 displays a slightly convex decay, the decrease observed in Cr<sub>2</sub>Ge<sub>2</sub>Te<sub>6</sub> is concave and shows a clear tendency to saturation at the highest pressures analyzed in this work. This behavior seems to go in hand with the pressure dependence of the magnetization at 10 K, which increases linearly with pressure for CrBr<sub>3</sub> (inset of Fig. 4a), but remains nearly constant above 0.6 GPa for Cr<sub>2</sub>Ge<sub>2</sub>Te<sub>6</sub>, inset of Fig. 4b.

As previously described, the electronic structure shows largely ionic  $Cr^{3+}$ : S = 3/2 cations with a half-filled spinpolarized  $t_{\mathrm{2g}}$  and  $e_{\mathrm{g}}$  manifold. This leads to a significant gap opening at the Fermi level for Cr<sub>2</sub>Ge<sub>2</sub>Te<sub>6</sub> and CrBr<sub>3</sub>, even at the LDA/GGA level, without the need to introduce strong correlation effects in the calculations. In a first approximation, this indicates that the magnetic semiconductor limit could be applicable to understand the pressure dependence of these systems. Note that for the case of Cr2Ge2Te6 we have only performed this analysis at pressures where the system remains a semiconductor. However, even if the system can be described in the localized limit, various different exchange interactions compete, responding differently to pressure, and this leads to a complex pressure dependence of  $T_{\rm C}$ . We have calculated the pressure dependence of both  $J_{\rm in}$  and  $J_{\rm out}$ . The system is fully relaxed at different volumes (including the lattice parameters c/aratio and the internal positions), and used the Birch-Murnaghan equation for obtaining the pressure value at each volume. 42 We set up a magnetic supercell combining different types of AF and FM couplings between the neighbouring Cr cations. The value of the magnetic exchange constants is obtained after subtraction of the total energy difference among various magnetic configurations, assuming these follow a simplistic Heisenberg-type spin Hamiltonian with neighbouring 3/2 spins for Cr as explained before. The results are summarized in Fig. 8. The ground state

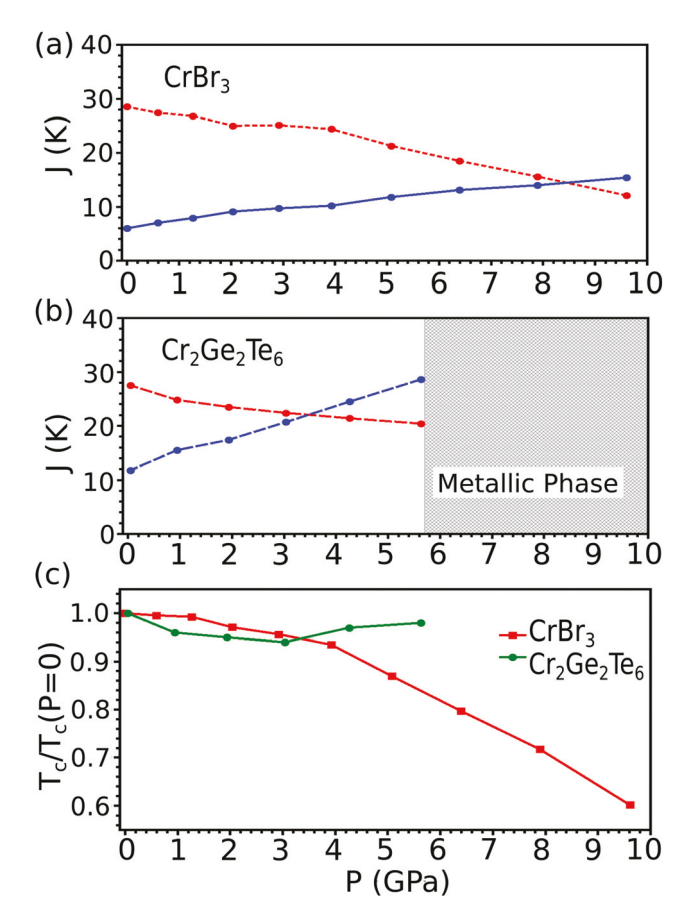


Fig. 8 (a) and (b) Values of the exchange constants extracted using a Heisenberg-type Hamiltonian for CrBr<sub>3</sub> and for Cr<sub>2</sub>Ge<sub>2</sub>Te<sub>6</sub>, respectively.  $J_{\rm out}$  in blue,  $J_{\rm in}$  in red. The out-of-plane coupling becomes larger as pressure is applied. (c) Evolution of the normalized transition temperature with pressure obtained from the Monte-Carlo simulation.

presents a FM coupling at low pressures, in agreement with experiments, but the different exchange constants behave differently with pressure, although all of them remain positive at all pressures, for both compounds.

With the calculated values of the magnetic exchange constants, we have set up a Heisenberg type Hamiltonian of interacting spins, and solved it using a classical Monte Carlo simulation. This allowed us to obtain a theoretical  $T_{\rm C}$  and its evolution with pressure. Despite the overestimation of the absolute value of magnetic exchange constants, the actual pressure dependence of the calculated  $T_{\rm C}$  is in good agreement with the observed experimental trend, as it can be seen from a comparison between Fig. 7a and 8c. In this figure, the theoretical values are normalized to the  $T_{\rm C}$  at ambient pressure. In the Heisenberg type Hamiltonian we have included an anisotropic term as in ref. 33, since it was reported that for Cr<sub>2</sub>Ge<sub>2</sub>Te<sub>6</sub> this term changes its sign with pressure. 43 However, no influence on the value of  $T_{\rm C}$  or its pressure dependence was observed due to the much smaller energy scale of the anisotropic term.

For  $CrBr_3$ ,  $J_{out}$  increases with pressure while  $J_{in}$  decreases (Fig. 8a). Since  $J_{\rm in} > J_{\rm out}$  and the number of Cr in-plane neighbours is greater than the out-of-plane, the trend of  $T_{\rm C}(P)$  is governed by  $J_{\rm in}$ . Therefore, decreasing  $J_{\rm in}$  produces the decrease of  $T_{\rm C}$  as pressure increases, in agreement with the experimental values in Fig. 7. On the other hand, for  ${\rm Cr_2Ge_2Te_6}$ ,  $J_{\rm out}$  increases with pressure, while, initially,  $J_{\rm in}$  decreases and saturates at higher pressure (see Fig. 8b). Therefore,  $J_{\rm in}$  dominates the change of  $T_{\rm C}$  at low pressures, but  $J_{\rm out}$  becomes the dominant term at higher pressures. This is in agreement with the experimental evolution presented for the  $T_{\rm C}$  with pressure (Fig. 7). Further experimental measurements at higher pressures should confirm the minimum in  $T_{\rm C}$  predicted in our calculations.

#### V. Conclusions

To summarize, pressure effects on the electronic, magnetic and structural properties of CrBr3 and Cr2Ge2Te6 have been explored following a combination of experimental and computational approaches. Our results show that CrBr3 is a Mott-Hubbard like insulator with a d-d energy gap. It follows that the system remains insulating under pressure. On the other hand, the energy gap of Cr<sub>2</sub>Ge<sub>2</sub>Te<sub>6</sub> is found to have p-d character, which leads to a charge transfer insulating behaviour. Our calculations predict an insulator to metal transition to occur at 6 GPa assuming no structural transition takes place. Despite the high pressure X-ray data shows a structural transition at similar pressures, whether this structural transition is accompanied with a softening of the lattice on approaching the putative insulator to metal transition or a mere structural change to a lower symmetry semiconducting state, cannot be concluded from our data. Additionally, resistivity measurements under pressure are needed to clarify this issue.

Besides, we have found that the different electronic structure of  $CrBr_3$  and  $Cr_2Ge_2Te_6$  and its evolution with pressure are at the root of the pressure dependence of the Curie temperature and the magnetic exchange interactions in  $Cr_2Ge_2Te_6$  and  $CrBr_3$ . The experimental observation yields a reduction of the Curie temperature as pressure is applied, in contrast to isostrucutral  $CrI_3$  and  $VI_3$ , but with a different trend for each compound. *Ab initio* calculations reveal that the microscopic origin for this trend relies on the different pressure dependence of the inand out-of-plane magnetic exchange couplings,  $J_{in,out} > 0$ .

While the transition temperature for  $CrBr_3$  is expected to monotonically decrease with pressure, the proximity of  $Cr_2Ge_2Te_6$  to the metallic limit yields a non-monotonic behavior. This effect was explained as a different behaviour of the inplane magnetic exchange coupling constants as a function of pressure for each compound.

This work sheds light on the competition of the different types of exchanges that may occur in several other quasi-two-dimensional magnetic materials. Similar competition between direct and indirect in-plane exchange paths and off-plane couplings may occur, such as the di- and trihalides. In fact, it might be at the origin of the presence or absence of magnetic ordering in the monolayer of transition metal phosphorus trisulfides (TMPS<sub>3</sub>) FePS<sub>3</sub> and NiPS<sub>3</sub>.<sup>44,45</sup> Long-range order

depends on the type of spin-spin interations, which themselves compete with intrinsic fluctuations and determine the magnetic anisotropy and the stability of long-range magnetic order at the monolayer limit. We have seen that in Cr-based van der Waals structures, these spin-spin interactions (and their competitions) are strongly dependent on the evolution of the electronic structure with pressure and, therefore reciprocally, on the dimensionality.

#### Conflicts of interest

There are no conflicts to declare.

#### Acknowledgements

This work was supported by the Spanish Government through Projects MAT2016-80762-R, PGC2018-101334-B-C21 and PGC2018-101334-A-C22. A. O. F. also through the FPU16/02572 grant. JSZ was supported by National Science Foundation grants DMR-1720595 and DMREF 1729588. ALBA synchrotron is acknowledged for provision of beamtime through the proposal number 2017092467. Xunta de Galicia (Centro singular de investigación de Galicia accreditation 2019-2022, ED431G 2019/03), the European Union (European Regional Development Fund - ERDF), and the European Commission through the project 734187-SPI-COLOST (H2020-MSCA-RISE-2016) are gratefully acknowledged.

#### References

- 1 K. S. Novoselov, A. K. Geim, S. V. Morozov, D. Jiang, Y. Zhang, S. V. Dubonos, I. V. Grigorieva and A. A. Firsov, Science, 2004, 306, 666.
- 2 K. F. Mak, C. Lee, J. Hone, J. Shan and T. F. Heinz, *Phys. Rev. Lett.*, 2010, **105**, 136805.
- 3 C. R. Dean, A. F. Young, I. Meric, C. Lee, L. Wang, S. Sorgenfrei, K. Watanabe, T. Taniguchi, P. Kim, K. L. Shepard and J. Hone, *Nat. Nanotechnol.*, 2010, 5, 722.
- 4 H. Liu, A. T. Neal, Z. Zhu, Z. Luo, X. Xu, D. Tománek and P. D. Ye, *ACS Nano*, 2014, **8**, 4033.
- 5 J.-U. Lee, S. Lee, J. H. Ryoo, S. Kang, T. Y. Kim, P. Kim, C.-H. Park, J.-G. Park and H. Cheong, *Nano Lett.*, 2016, 16, 7433, DOI: 10.1021/acs.nanolett.6b03052.
- 6 W.-B. Zhang, Q. Qu, P. Zhu and C.-H. Lam, *J. Mater. Chem. C*, 2015, 3, 12457.
- 7 Z. Fei, B. Huang, P. Malinowski, W. Wang, T. Song, J. Sanchez, W. Yao, D. Xiao, X. Zhu, A. F. May, W. Wu, D. H. Cobden, J.-H. Chu and X. Xu, *Nat. Mater.*, 2018, 17, 778.
- 8 D. Ghazaryan, M. T. Greenaway, Z. Wang, V. H. Guarochico-Moreira, I. J. Vera-Marun, J. Yin, Y. Liao, S. V. Morozov, O. Kristanovski, A. I. Lichtenstein, M. I. Katsnelson, F. Withers, A. Mishchenko, L. Eaves, A. K. Geim, K. S. Novoselov and A. Misra, *Nat. Electron.*, 2018, 1, 344.
- 9 D. R. Klein, D. MacNeill, J. L. Lado, D. Soriano, E. Navarro-Moratalla, K. Watanabe, T. Taniguchi, S. Manni, P. Canfield,

- J. Fernández-Rossier and P. Jarillo-Herrero, Science, 2018, 360, 1218,
- 10 B. Huang, G. Clark, D. R. Klein, D. MacNeill, E. Navarro-Moratalla, K. L. Seyler, N. Wilson, M. A. McGuire, D. H. Cobden, D. Xiao, W. Yao, P. Jarillo-Herrero and X. Xu, Nat. Nanotechnol., 2018, 13, 544.
- 11 Y. Cao, V. Fatemi, A. Demir, S. Fang, S. L. Tomarken, J. Y. Luo, J. D. Sanchez-Yamagishi, K. Watanabe, T. Taniguchi, E. Kaxiras, R. C. Ashoori and P. Jarillo-Herrero, Nature, 2018, 556, 80.
- 12 J. B. Goodenough, Magnetism and the chemical bond, IEEE Press, New York, 2001.
- 13 M. A. McGuire, H. Dixit, V. R. Cooper and B. C. Sales, Chem. Mater., 2015, 27, 612.
- 14 Y. Gao, J. Wang, Z. Li, J. Yang, M. Xia, X. Hao, Y. Xu and F. Gao, Phys. Status Solidi RRL, 2019, 13, 1800410, DOI: 10.1002/pssr.201800410.
- 15 Y. Zhao, L. Lin, Q. Zhou, Y. Li, S. Yuan, Q. Chen, S. Dong and J. Wang, Nano Lett., 2018, 18, 2943.
- 16 Y. Gao, J. Wang, Y. Li, M. Xia, Z. Li and F. Gao, Phys. Status Solidi RRL, 2018, 12, 1800105, DOI: 10.1002/pssr.201800105.
- 17 V. Carteaux, D. Brunet, G. Ouvrard and G. Andre, J. Phys.: Condens. Matter, 1995, 7, 69.
- 18 I. Tsubokawa, J. Phys. Soc. Jpn., 1960, 15, 1664, DOI: 10.1143/ JPSJ.15.1664.
- 19 W. Xing, Y. Chen, P. M. Odenthal, X. Zhang, W. Yuan, T. Su, Q. Song, T. Wang, J. Zhong, S. Jia, X. C. Xie, Y. Li and W. Han, 2D Mater., 2017, 4, 024009.
- 20 Z. Zhang, J. Shang, C. Jiang, A. Rasmita, W. Gao and T. Yu, Nano Lett., 2019, 19, 3138, DOI: 10.1021/acs.nanolett.9b00553.
- 21 P. Hohenberg and W. Kohn, Phys. Rev., 1964, 136, B864.
- 22 R. O. Jones and O. Gunnarsson, Rev. Mod. Phys., 1989, **61**, 689.
- 23 K. Schwarz and P. Blaha, Comput. Mater. Sci., 2003, 28, 259.
- 24 E. Sjöstedt, L. Nördstrom and D. J. Singh, Solid State Commun., 2000, 114, 15.
- 25 F. Tran, J. Stelzl, D. Koller, T. Ruh and P. Blaha, Phys. Rev. B, 2017, 96, 054103.
- 26 J. P. Perdew, K. Burke and M. Ernzerhof, Phys. Rev. Lett., 1996, 77, 3865.
- 27 N. Metropolis, A. W. Rosenbluth, M. N. Rosenbluth, A. H. Teller and E. Teller, J. Chem. Phys., 1953, 21, 1087, DOI: 10.1063/ 1.1699114.
- 28 M. D. Kuz'min, Phys. Rev. Lett., 2005, 94, 107204.

- 29 A. Barla, J. Nicolás, D. Cocco, S. M. Valvidares, J. Herrero-Martn, P. Gargiani, J. Moldes, C. Ruget, E. Pellegrin and S. Ferrer, J. Synchrotron Radiat., 2016, 23, 1507.
- 30 E. Gaudry, A. Kiratisin, P. Sainctavit, C. Brouder, F. Mauri, A. Ramos, A. Rogalev and J. Goulon, Phys. Rev. B: Condens. Matter Mater. Phys., 2003, 67, 094108.
- 31 M. W. Haverkort, M. Zwierzycki and O. K. Andersen, Phys. Rev. B: Condens. Matter Mater. Phys., 2012, 85, 165113.
- 32 Y. Lu, M. Höppner, O. Gunnarsson and M. W. Haverkort, Phys. Rev. B: Condens. Matter Mater. Phys., 2014, 90, 085102.
- 33 C. Gong, L. Li, Z. Li, H. Ji, A. Stern, Y. Xia, T. Cao, W. Bao, C. Wang, Y. Wang, Z. Q. Qiu, R. J. Cava, S. G. Louie, J. Xia and X. Zhang, Nature, 2017, 546, 265.
- 34 D. J. Singh, Phys. Rev. B: Condens. Matter Mater. Phys., 2007, 76, 085110.
- 35 Z. Yu, W. Xia, K. Xu, M. Xu, H. Wang, X. Wang, N. Yu, Z. Zou, J. Zhao and L. Wang, et al., J. Phys. Chem. C, 2019, 123, 13885.
- 36 H. Yoshida, J. Chiba, T. Kaneko, Y. Fujimori and S. Abe, Phys. B, 1997, 237-238, 525, proceedings of the Yamada Conference XLV, the International Conference on the Physics of Transition Metals.
- 37 Y. Sun, R. C. Xiao, G. T. Lin, R. R. Zhang, L. S. Ling, Z. W. Ma, X. Luo, W. J. Lu, Y. P. Sun and Z. G. Sheng, Appl. Phys. Lett., 2018, 112, 072409, DOI: 10.1063/1.5016568.
- 38 W. A. Harrison, Electronic Structures and the Properties of Solids: The Physics of the Chemical Bond, Dover Publications Inc., New York, 1988.
- 39 D. Bloch, J. Phys. Chem. Solids, 1966, 27, 881.
- 40 S. Blanco-Canosa, F. Rivadulla, V. Pardo, D. Baldomir, J.-S. Zhou, M. García-Hernández, M. A. López-Quintela, J. Rivas and J. B. Goodenough, Phys. Rev. Lett., 2007, 99, 187201.
- 41 S. Blanco-Canosa, F. Rivadulla, A. Piñeiro, V. Pardo, D. Baldomir, D. I. Khomskii, M. M. Abd-Elmeguid, M. A. López-Quintela and J. Rivas, Phys. Rev. Lett., 2009, 102, 056406.
- 42 F. Birch, Phys. Rev., 1947, 71, 809.
- 43 Z. Lin, M. Lohmann, Z. A. Ali, C. Tang, J. Li, W. Xing, J. Zhong, S. Jia, W. Han, S. Coh, W. Beyermann and J. Shi, Phys. Rev. Mater., 2018, 2, 051004.
- 44 J.-U. Lee, S. Lee, J. H. Ryoo, S. Kang, T. Y. Kim, P. Kim, C.-H. Park, J.-G. Park and H. Cheong, Nano Lett., 2016, 16, 7433.
- 45 K. Kim, S. Y. Lim, J.-U. Lee, S. Lee, T. Y. Kim, K. Park, G. S. Jeon, C.-H. Park, J.-G. Park and H. Cheong, Nat. Commun., 2019, 10, 1.